Environment International 169 (2022) 107490

Contents lists available at ScienceDirect

Environment International

journal homepage: www.elsevier.com/locate/envint

Full length article

Impact of mining on the metal content of dust in indigenous villages of northern Chile

Nicolás C. Zanetta-Colombo [a,b,c,*], Zoë L. Fleming [d,e], Eugenia M. Gayo [e,f], Carlos A. Manzano [g,h,*], Marios Panagi [i], Jorge Valdés [j], Alexander Siegmund [a,b]

[a] Heidelberg Center for the Environment (HCE), Heidelberg University, Heidelberg, Germany
[b] Department of Geography – Research Group for Earth Observation (rgeo), Heidelberg University of Education, Heidelberg, Germany
[c] Department of Geography, SAI, Heidelberg University, Heidelberg, Germany
[d] Envirohealth Dynamics Lab, C+ Research Center in Technologies for Society, School of Engineering, Universidad Del Desarrollo, Santiago, Chile
[e] Center for Climate and Resilience Research (CR)2, Chile
[f] ANID – Millennium Science Initiative Program– Nucleo Milenio UPWELL, Chile
[g] Departamento de Química, Facultad de Ciencias, Universidad de Chile, Santiago, Chile
[h] School of Public Health, San Diego State University, San Diego, CA, USA
[i] School of Physics and Astronomy, University of Leicester, Leicester, UK
[j] Laboratorio de Sedimentología y Paleoambientes (LASPAL), Instituto de Ciencias Naturales Alexander von Humboldt, Facultad de Ciencias del Mar y de Recursos Biológicos, Universidad de Antofagasta, Antofagasta, Chile

ARTICLE INFO

Handling Editor: Adrian Covaci

Keywords:
Toxic metal
Mining emissions
Pollution risk
Health risk assessment
Atacama

ABSTRACT

Indigenous communities from northern Chile have historically been exposed to the impacts of massive copper industrial activities conducted in the region. Some of the communities belonging to the Alto El Loa Indigenous Development Area are located less than 10 km from the "Talabre'' tailings dam, which contains residues from copper production and other metals that can be toxic to human health (e.g., As, Sb, Cd, Mo, Pb). Given the increasing demand of copper production to achieve net-zero emission scenarios and concomitant expansions of the tailings, the exposure to toxic metals is a latent risk to local communities. Despite the impact that copper production could generate on ancestral communities from northern Chile, studies and monitoring are limited and the results are often not made accessible for local communities. Here, we evaluate such risks by characterizing metal concentrations in dust collected from roofs and windows of houses from the Alto El Loa area. Our results showed that As, Sb, Cd, Cu, Mo, Ag, S, and Pb concentrations in these matrices can be connected to local copper mining activities. Additionally, air transport models indicate that high concentrations of toxic elements (As, Sb, and Cd) can be explained by the atmospheric transport of particles from the tailings in a NE direction up to 50 km away. Pollution indices and Health Risk Assessment suggested a highly contaminated region with a health risk for its inhabitants. Our analysis on a local scale seeks to make visible the case of northern Chile as a critical territory where actions should be taken to mitigate the effects of mining in the face of this new scenario of international demand for the raw materials necessary for the transition to a net-zero carbon global society.

1. Introduction

Copper has become a key metal for the technological development of global modern societies. Over the next few decades, its relevance will increase, spurred on by the urgency of achieving carbon neutrality (Schipper et al., 2018). The demand for copper is expected to increase by 275–350% by 2050 (Elshkaki et al., 2016). Although this will certainly align with many of the Sustainable Development Goals (SDGs) set by the United Nations for 2030, such a situation could lead to new socio-environmental conflicts, particularly in developing regions of the world in which the increased extraction and production of copper and other metals could have a direct effect on some of the SDGs at a local scale: well-being, equality, access to clean water and sanitation, among others (Zografos and Robbins, 2020).

* Corresponding authors at: Heidelberg Center for the Environment (HCE), Heidelberg University, Heidelberg, Germany (N.C. Zanetta-Colombo). Departamento de Química, Facultad de Ciencias, Universidad de Chile, Santiago, Chile (C.A. Manzano).
E-mail addresses: nicolas.zanetta@stud.uni-heidelberg.de (N.C. Zanetta-Colombo), carlos.manzano@uchile.cl (C.A. Manzano).

https://doi.org/10.1016/j.envint.2022.107490
Received 14 April 2022; Received in revised form 29 July 2022; Accepted 22 August 2022
Available online 24 August 2022

One of the most important impacts of copper mining on surrounding local communities is the trace element pollution brought about by dust emissions either from ore extraction, high-temperature processing, and tailings disposal (Csavina et al., 2012). Especially, from the emission of non-essential trace elements or potentially toxic elements (PTE) even at low concentrations (e.g., As, Cd, Sb, Pb, Hg, among others) (Pourret et al., 2021). PTEs represent a significant risk to ecosystems and human health as they are considered persistent pollutants that bioaccumulate in organisms throughout the food chain (Khan et al., 2015; Sall et al., 2020). Additionally, the exposure to some PTEs such as As and Pb are associated with a wide array of chronic diseases, neurological and neurobehavioral disorders, increased cancer risk, as well as developmental abnormalities (Tchounwou et al., 2003; Thomas et al., 2009). The impact of copper mining has been documented in the Americas (Zapata, 2020; Moya et al., 2019), Oceania (Mudd et al., 2020), Africa (Wilson et al., 2017), Asia (Monjezi et al., 2009; Pandey et al., 2007), and Europe (Lilic et al., 2018; Song et al., 2017). However, more studies are needed in rural areas of the global south, a region with large copper deposits yet to be explored.

Chile has a long mining tradition since pre-Columbian times, with a sustained industrial development since the 16th century (Gayo et al., 2019). Today, it is the world's largest copper producer (27% of global production in 2021) through massive operations concentrated in the northern and central regions of the country (19°–33°S). The processes

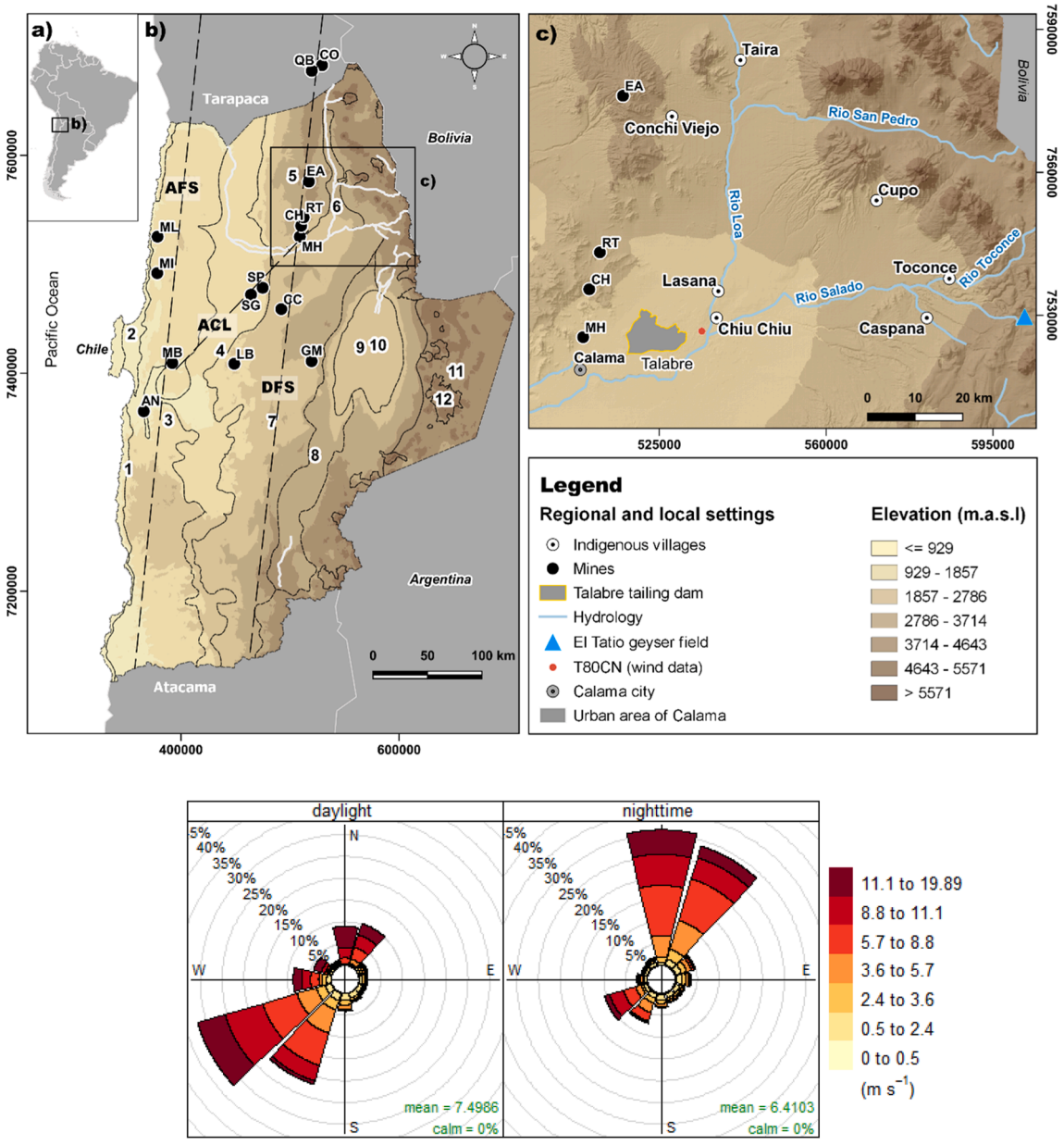

Fig. 1. Regional and local settings. The map shows a) the location of the Antofagasta Region in the Chilean and South American context. b) Geomorphologic units (numbers) are shown, as well as the location of the primary mining operations (black dots). In b) numbers allude to (1) Coastal escarpment, (2) Coastal plain, (3) Coastal range, (4) the Atacama Desert, (5) Precordillera, (6) Loa depression, (7) Domeyko range, (8) Inter-range basins, (9) Cordillera de la Sal, (10) Salar de Atacama basin, (11) Altiplano, (12) Active volcanoes. The dotted lines represent the approximate location of the Atacama Fault System (AFS), the Domeyko Fault System (DFS), and the Antofagasta-Calama Lineament (ACL). c) Study area and the indigenous communities where samples were taken with the Chuquicamata (CH), Ministro Hales (MH), Radomiro Tomic (RT), and El Abra (EA) mining operations shown. d) Wind Roses for Calama Norte (T80CN) showing the frequency of counts by wind direction (%) and wind speed (m s^{-1}), separated into daylight and nighttime hours. The website http://walker.dgf.uchile.cl/Mediciones/ was run for 2011-02-21 to 2012-12-27.

involved in metal mining (i.e., excavation, crushing, grinding, separation, smelting, refining, and tailings management) are a large anthropogenic source of PTEs on a national scale, representing 98% of all emissions in the country (Zhu et al., 2020), which have increased with the recent expansion of production and exports (Cerda et al., 2019; Eichler et al., 2015, 2017; Gayo et al., 2019; Schwanck et al., 2016; Vleeschouwer et al., 2014).

The study of the potential impacts of PTE emissions in Chile has focused on urban areas (Madrid et al., 2022; Muñoz et al., 2019; Tapia et al., 2018), while rural areas have been poorly addressed. This has created an important gap of information in mining regions, in which socio-environmental conflicts have emerged (Manzano et al., 2021; Romero-Toledo, 2019; Tapia et al., 2018; Zang et al., 2018).

Located between the hyperarid Atacama Desert and the Andean mountains (Fig. 1), Alto El Loa is the leading mining center in the country and one of the most important in Latin America. Here, the Chuquicamata mine (once considered the largest open-pit mine in the world) has developed its industrial activity since the beginning of the 20th century, and other large industrial facilities such as Radomiro Tomic, El Abra, Collahuasi, and Ministro Hales have been operating since the 1990s. Moreover, the country's largest tailing dam (Talabre, ~60 km^2) is also located in this area.

Alto El Loa is an Indigenous Development Area (IDA), a protection figure that the Chilean government implemented in 1995 in order to protect the quality of life of its native people (Vergara et al., 2006), and it is the most illustrative example of the socio-environmental tensions between indigenous communities (Atacameño, Quechua, and Aymaras) and mining companies (Carrasco, 2015) which has been fuelled by the expansion of mining operations in response to the prevailing neoliberalist (extractivism) economic model of Chile (Smart, 2017). Despite the demands of communities for more clarity about the consequences of mining operations on human and environmental health, no public environmental monitoring has been implemented so far, and much of the information derives from a few sparse studies (De Gregori et al., 2003; González-Rojas et al., 2021).

This study aims to evaluate the potential impacts of the local mining industry on the IDA territory by analysing concentrations and spatio-temporal patterns in the distribution of PTEs. We provide the first insight into local levels of environmental contamination (i.e., pollution levels and enrichment factors) as well as potential exposure to PTEs via ingestion. We focused on settled dust as this environmental matrix offers the means to assess the population's exposure to potentially toxic elements in outdoor (Moya et al., 2019; Rout et al., 2013; Tapia et al., 2018; Taylor et al., 2014) and in indoor environments (Gohain and Deka, 2020; Shi and Wang, 2021; Yang et al., 2015). More importantly, in areas where official environmental monitoring is limited or absent, this inexpensive approach allows an assessment of pollution sources, their intensity and potential impacts. Additionally, since the impact of mining operations does not solely rely on the quantity and toxicity of emissions (Csavina et al., 2012), but also on dispersion processes, we evaluated the potential for atmospheric transport of air pollution which can be indicative of the quantity and type of settled dust in the IDA.

2. Materials and methods

2.1. Sampling area

The Antofagasta Region, in the North of Chile, has a total population of 607,504 inhabitants (INE, 2018). This region has undergone significant transformations in recent decades, mainly because of the expansion of large-scale mining operations, which has affected other traditional agricultural practices, increasing rural-to-urban migration (Calderón-Seguel et al., 2021). The largest urban center in the region is the city of Calama, which has a population of 165,731, approximately 98% of which are located in urban centers, while less than 2% are located in rural areas (INE, 2018).

The region has a hyper arid climate with two sources of humidity. During the austral summer (December – February), northeastern (monsoonal) air flows from the Amazon, leading to allowing rain and snow (Houston and Hartley, 2003). Extreme events associated with La Niña usually generate floods in the area. During austral winter (June – August), south westerly airflows bring frontal precipitation from extra-tropical cyclones, where extreme events tend to be associated with El Niño (Houston, 2006).

Precipitation, although scarce, increases with altitude, with an average annual precipitation of 4.2 mm in Calama and 63.3 mm in Caspana (see their locations in Fig. 1c) with significant contributions of summer rains in the upper part of the basin (Houston, 2006).

There is a strong diurnal variability in wind speed and direction. Northerly down-valley wind direction occurs during the night, while westerly upslope flows are characteristic during the daytime (Muñoz et al., 2018; González-Rojas et al., 2021) (Fig. 1).

The Loa River, the longest in Chile 440 km, originates in this area (at 3950 m a.s.l.) and extends westward to the Pacific Ocean, creating an important green corridor that crosses the hyper-arid core of the Atacama Desert. The Loa River flow has progressively decreased over the past decades because of the intensive exploitation of the aquifers adjacent to it by mining activities, affecting the indigenous communities and the native flora and fauna (Herrera et al., 2021). The Loa River receives surface and groundwater contributions from the Salado River in its upper course, near Chiu Chiu. The Salado River (Fig. 1c), which in turn is a tributary of the El Tatio geothermal field, has been studied for its high concentrations of As, which has led it to be considered the primary source of this toxic metal in the Loa basin (Romero et al., 2003).

Geological background and geomorphological units: In northern Chile, the occurrence of the porphyry Cu and porphyry-related mineral deposit and their spatial distribution is strongly associated with the eastward-migrating tectonic-magmatic activities, controlled by the Atacama and Domeyko fault system (Zhu and Lu, 2016). In the Antofagasta Region, the Coastal Cordillera, a Carboniferous – Early Triassic magmatic arc, contains numerous copper deposits from the Upper Jurassic, such as Mantos Blancos (Ramírez et al., 2006). Tracking the displacement of tectonic activity, a Paleocene-early Eocene belt of porphyry copper deposits is situated within the Central Depression, where the Spence deposit stands out as part of the Antofagasta – Calama Lineament (Palacios et al., 2007). Slightly further east, a late Eocene-early Oligocene belt is hosted by rocks of the Precordillera, which occur along the Domeyko Fault Zone (DFZ) (Fig. 1b). During the structural and geomorphological evolution of the Precordillera, some deposits have been exhumed and exposed at the surface (Cameron et al., 2008), such as the Chuquicamata porphyry Cu (Mo-Ag) deposit. Controlled by the initial intrusions (~36–33 Ma) through mineralization to post-mineral brecciation and offset by the West fault system (Ossandon et al., 2001), Chuquicamata has been exploited since pre-colonial times (Fuller, 2004) and is the world's greatest copper orebody. The Calama basin, located between 2000 and 3500 m a.s.l. (22° – 23° S), is a mid-elevation sedimentary plateau covering approximately 2000 km^2. Most of the indigenous villages of Alto El Loa are situated within this basin, usually within or close to the deep river canyons that form natural oases and shelters from the persistent winds.

Mining and Talabre tailings: The Talabre tailings have their orig in the Chuquicamata porphyry copper deposits (Smuda et al., 2014). Th primary minerals extracted are sulfides (including pyrite (FeS_2), bornite (Cu_5FeS_4), chalcopyrite ($CuFeS_2$), and digenite ($CuAsS_4$)) among others. After crushing and milling, the ore is treated chemically to separate the ore from secondary elements and impurities. 80% of the water used in the process is obtained from the Loa River and 20% from the water recovered from the tailing after the flotation process. With an average tailing deposition of about 200,000 t/day, the total volume of the Talabre impoundment is approx. 600,000 m^3 and in 2009 covered a total surface area of 52 km^2 (Smuda et al., 2014). Once the sedimentation reaches 3 m in the tailing, the discharge point is shifted to another

basin and subsequently, water-saturation decreases due to drainage and evaporation, forming unsaturated vadose zones, exposing dry sediments that could be lifted by winds.

2.2. Sample collection, processing, and analysis

A social participative sampling methodology was used, allowing local people to accompany the process and, after having a brief training by the researchers, participate in the sampling process. It has been proposed that simple local engagement, including active collaborations and codesign of strategies, can alleviate what has been called the environmental belief paradox (the disparity between the level of concern and engagement of affected communities in environmental justice issues) (Dietz and Whitley, 2018; Pearson et al., 2018). Allowing the community to be part of the scientific process can help us develop shared perspectives on the problem they are facing, and promote pro-environmental behaviour.

The sampling points were selected based on community relevance (e.g., schools and community centers) and were often suggested by locals. Outdoor dust was collected between January 5 and January 8, 2021. Twenty-nine samples were collected from the roofs and windowsills (from now on referred to as "windows") in seven indigenous villages of Alto El Loa: Lasana (La, n = 5), Chiu Chiu (Ch, n = 6), Conchi Viejo (Cv, n = 4), Taira (Ta, n = 4), Cupo (Cu, n = 2), Caspana (Ca, n = 4), and Toconce (To = 4) located within a radius of 60 km from Talabre and Chuquicamata (Fig. 1). A synthetic bristle brush, washed with distilled water after each sampling, was used to sweep accumulated dust into a polypropylene container. Similar methods have been previously used to report trace metals concentrations in deposited dust in roofs near industrial areas in South Korea (Lee et al., 2020), China (Yu et al., 2017), and Peru (Chui Betancur et al., 2016); and in roads near urban centers (Trujillo-González et al., 2016; Amato et al., 2009). Each sample was composed of at least three subsamples of the same type and sector to increase representativeness. In addition, surface soil samples of 2 cm depth (collation of 6 samples collected with stainless steel spoons from a 1 m^2 area) were collected in the dust sampling sites to obtain a vertical gradient (roof – windows – soil). For reasons of force majeure, no soil samples were collected in the village of Chiu Chiu. The geographical positions of sampling sites were measured by a portable GPS (Garmin Etrex 30 model). The geographical coordinates of all sampling sites can be found in the supplemental information (Table S1).

Sample processing was carried out in the Faculty of Engineering at the Universidad del Desarrollo (UDD) in Santiago, Chile. Samples were dried in an oven (1 hr. at 100 °C) and sieved to the < 75 μm fraction with a stainless steel mesh standard testing sieve (ASTM E-11/2009) to separate the coarser particles and components that could interfere with further analysis. The sieve was washed with demineralized water after sieving each sample to avoid cross-contamination. Particles below 75 μm in diameter are conventionally considered "dust", and this fraction has been widely used for health risk assessment in populations exposed to potential contaminants, mainly through ingestion routes (Zhao et al., 2016; Fan et al., 2022; Malakootian et al., 2021). Additionally, some studies indicate that this fraction can contain relatively high metal concentrations (Kolakkandi, et al., 2020; Förstner and Salomons, 1980; Horowitz et al., 1990).

A subset (0.2 g) of the < 75 μm fraction was digested in 20 ml of a multi-acid (5 ml HNO_3, 2.5 ml $HClO_4$, 10 ml HF, 5 ml HCl/ 20% HCl) and analysed using Inductively Coupled Plasma Optical Emission Spectrometry (ICP-OES, PerkinElmer Avio® 500) with spectral corrections using an ion-exchange chromatography (IEC) model. Blank and standard reference materials (OREAS 153b and OREAS 602, Melbourne, Australia) were used for quality assurance and quality control (Table S2). Elemental analyses were made at the certified laboratory: SGS Minerals S.A. in Santiago, Chile. The analysis focused on the determination of elements potentially coming from mining activities in rural areas of northern Chile, and thus, other abundant crustal elements and markers of traffic emissions were not measured. The detection limits for each element are included in the results in Table 1.

2.3. Statistical methods

Descriptive statistics (i.e., mean, standard deviation, skew, kurtosis), and the coefficient of variation (CV), were used to categorize and describe the distribution of elements in the study area. Similar approaches have been used in other urban environments worldwide (Hou et al., 2019; Doyi et al., 2019; Fan et al., 2022). The CV was calculated to compare the variability of the metal concentration from the total settled dust. According to previous studies, the CV was categorized into four classes: CV ≤ 20% was regarded as low variability, 21% < CV > 50% indicated moderate variability, 51% < CV ≤ 100% as regarded as high variability, and CV > 100% was considered very high variability.

The Spearman correlation coefficients were calculated to determine correlations among elements, while principal component analysis (PCA) was conducted to explore further connections.

2.4. Potential transport of dust particles

Potential for dust resuspension at Talabre: The tailings discharge at Talabre consists of 45.1 wt% solids and 54.9 wt% water (Smuda et al., 2014). High levels of solar radiation and limited surface humidity favor high evaporation, which decreases the water content of the tailings, leaving dry material available on the surface that can be subjected to atmospheric transport. The Normalized Difference Water Index (NDWI) was calculated for the Talabre tailing dam for 127 days between 2018 and 2020, using the threshold (>0.015) for wet tailing proposed by (Hao et al., 2019). NDWI was calculated by Google Earth Engine and Landsat 7, using the following formula:

$$NDWI = \frac{G - NIR}{G + NIR} \quad (1)$$

where NIR is the spectral reflectance in the Near Infra-red Band (Band 8), and G is the spectral reflectance in the Green Band (Band 3).

Dispersion modelling: The Numerical Atmospheric Modelling Environment (NAME) model, created by the UK Met Office (Jones et al., 2007) was used to plot air mass footprints that show the dispersion of the air that passes over the surface of the mine and its transport for the next 9 h. NAME uses meteorological fields from the Unified Model (Brown et al., 2012), to track the pathways of hypothetical inert tracers. The fields used in this study had a resolution of 0.23° longitude by 0.16° latitude with 59 vertical levels up to an approximate height of 30 km. 3-hourly footprints were modelled for the whole of 2020 for 9 h forwards (since already after this time many air masses have already crossed the border to Bolivia) from Talabre on a 0.05° × 0.05° resolution, focussing on the layer from 0 to 100 m above the surface, thus taking into account when substances or emissions could be picked up from a surface and when they could reappear on the surface further afield. The models were carried out in an objective way, taking into account a long-lived tracer (with CO as the tracer) and estimating the potential extent of transport of any air mass. The run was done without knowledge of chemical composition and without any knowledge of suspension or deposition of particulate matter, making it an objective view on the potential extent of influence of winds from one area to another. The units were based on a release of a known quantity of air masses (hypothetical particles) in grams (g) during an integrated time-period (s) and the results are displayed per grid box, which has a volume component.

2.5. Risk assessment

Enrichment factors and Geoaccumulation index: The enrichment factor (EF) and the index of geoaccumulation (I_{geo}) were applied to assess metal concentrations and distribution in the settled dust of the

Table 1
Descriptive statistics and basic testing for metals in total settled dust. The Coefficient of Variability that displays the variability in the measurements between sites is graded by (*) with *** showing the highest variability, then ** and then *. Those without * showed little variation, suggesting there was little anthropogenic influence.

Metal	Al	Fe	S	Ti	Cu	Zn	As	V	Pb	Mo	Cr	Ni	Co	Sb	Cd	Ag
Unit	%	%	%	%	%	mg kg^{-1}	mg kg^{-1}	mg kg^{-1}	mg kg^{-1}	mg kg^{-1}	mg kg^{-1}	mg kg^{-1}	mg kg^{-1}	mg kg^{-1}	mg kg^{-1}	mg kg^{-1}
ns total	29	29	29	29	29	29	29	29	29	29	29	29	29	25	15	26
DL	0.01	0.01	0.01	0.01	0.01	1	1	1	1	2	1	1	1	2	1	0.5
ns BDL	–	–	–	–	–	–	–	–	–	–	–	–	–	4	14	3
mean	7.3	4.1	0.6	0.5	0.2	2352.1	197.8	131.4	101.9	79	42	16.2	14.4	12.1	2.6	2.4
sd	0.6	0.6	0.4	0.1	0.2	3324.7	137.9	18.1	63.2	80	17.8	2.2	5.3	9.7	1.6	2.1
median	7.5	4	0.5	0.5	0.2	547	147	130	88	65	36	16	13	9	2	1.7
min	6.2	3.1	0.2	0.3	n.d.	159	67	104	25	5	25	13	10	2	1	0.5
max	8.4	5.7	1.6	0.7	0.7	12,498	564	204	221	338	119	23	39	38	6	8.9
range	2.2	2.6	1.4	0.4	0.7	12,339	497	100	196	333	94	10	29	36	5	8.4
skew	−0.3	0.9	1.5	1.1	0.8	1.5	1.4	2.1	0.5	1.5	2.8	1.1	3.4	1.3	0.8	1.5
kurtosis	−0.8	0.9	1.1	2.1	−0.6	1.2	0.9	6.5	−1.2	2	9.4	1.2	12.6	0.8	−0.9	1.7
CV (%)	8	14	65**	18	78**	141***	70**	14	62	101***	42*	13	37*	80**	63**	89**

villages of Alto El Loa, relative to the regional background levels, following equations (2) and (3).

$$EF = \frac{\left(\frac{M}{X}\right)_{sample}}{\left(\frac{M}{X}\right)_{background}} \quad (2)$$

$$I_{geo=}\frac{C_n}{1.5*B_n} \quad (3)$$

where M is the concentration of the metal being analysed and X is the concentration of the reference element; and where C_n is the measured concentration of metal, B_n is the geochemical background, and a factor of 1.5 is used to include the possible variation of background values due to lithogenic effects (Müller, 1979).

An element with low variability of occurrence is used as a reference for the EF. Typically, Al, Fe, Mn, or Rb are used as reference elements, which should not have a direct anthropogenic source. Since Mn and Rb were not measured in this study, and Al is a major component of the roofs sampled (55% Al: 43.4% Zn: 1.6% Si), we used Fe as the reference element (Fe showed the second lowest variability in the study area, CV: 14%). If the EF ranges from 0.5 to 1.5, natural weathering processes or crustal materials might be influencing this concentration. However, if the values exceed 1.5, there is a possibility that the trace metal contamination occurred because of anthropogenic activities. Pollution levels of EF were classified as: deficiency to minimal enrichment ($EF < 2$), moderate enrichment ($2 < EF < 5$), significant enrichment ($5 < EF < 20$), very high enrichment ($20 < EF < 40$), and extremely high enrichment ($EF > 40$) (Barbieri, 2016).

The I_{geo} index was evaluated following the scale proposed by Müller (1981): unpolluted (Igeo < 0), unpolluted to moderately polluted ($0 < I_{geo} < 1$), moderately polluted ($1 < I_{geo} < 2$), moderately to strongly polluted ($2 < I_{geo} < 3$), strongly polluted ($3 < I_{geo} < 4$), very strongly polluted ($4 < I_{geo} < 5$), and extremely polluted ($5 < I_{geo}$). This study used the average background values for the Antofagasta Region, composed of 17 soil samples collected in pollution-free zones (Fig. S1) by the Chilean National Center for the Environment (CENMA, 2014).

Health Risk Assessment: The health risk assessment model proposed by the United States Environmental Protection Agency (US EPA) was applied to quantify the potential non-carcinogenic and carcinogenic risk from ingesting settled dust by children in Alto El Loa (US EPA, 1989; US EPA, 2009; US EPA, 2013).

$$ADD = \frac{(Ci \times IngR \times EF \times ED)}{(BW \times AT)} \times 10^{-6} \quad (4)$$

where *ADD* is the average daily intake doses (mg kg^{-1} day^{-1}); *C* represents the PTE concentrations in settled dust (mg kg^{-1}); *IngR* is the recommended central tendency of settled dust ingestion rates for children (200 mg day^{-1} for the age < 6 including soil and outdoor dust (US EPA, 2009)); *EF* is the exposure frequency of 365 days $year^{-1}$ (assuming children spending all the time in their villages); *ED* is the exposure duration (6 years for children is assumed in this study), equivalent to the average lifetime (Huang et al., 2008); *BW* is the average body weight in kg (18.6 kg average for the range 3 to < 6 years) (US EPA, 2009); and *AT* is the averaging time estimated as the *ED* * 365 days. This is a well-known method that has provided important information on the potential health risk associated with contaminated areas worldwide (Kurt-Karakus, 2012; Hou et al., 2019; Doyi et al., 2019; Fan et al., 2022). It was calculated for children, who are likely to ingest more through their playing habits and who are more susceptible to the effects of pollution as their organism is still growing and developing.

Potential non-carcinogenic risk related to specific PTE were then assessed using Hazard Quotient (HQ) according to the Eq. (5).

$$HQ = \frac{ADD}{RfD} \quad (5)$$

where *RfD* (mg/kg/day) indicates the oral reference dose of PTE as suggested by US EPA (3×10^{-4} for As, 1×10^{-3} for Cd, 4×10^{-4} for Sb, 4×10^{-2} for Cu, 5×10^{-3} for Mo, 5×10^{-3} for Ag). The US EPA has not established an *RfD* for Pb, but was derived from published studies (1.4×10^{-3}) (Cao et al., 2015). If the *HQ* is greater than 1, there may be concern for potential adverse non-cancer health effects. The greater the value of *HQ*, the greater the level of concern (Huang et al., 2008). Considering that the exposure to more than two pollutants can result in an additive effect, the Hazard Index (*HI*), the sum of individual *HQ*, was calculated (Eq. (6)) to assess the overall potential of non-carcinogenic effects posed by more than one PTE. If $HI < 1$ then no significant risk occurs, but when $HI > 1$ chronic risk is more likely to occur.

$$HI = \sum_{i=i}^{n} HQ \quad (6)$$

Carcinogenic risk (*CR*) indicates the possibility of an individual developing any kind of cancer due to exposure to carcinogenic hazards (US EPA, 1989). The *CR* of As and Cd, both carcinogenic elements, were calculated according to Eq. (7).

$$CR = ADDxSF \quad (7)$$

where SF (mg/kg body per day)$^{-1}$ refers to the slope factor which is 1.5 for As and 6.1 for Cd. If the risk is higher than the threshold value of $1 \times 10^{-4} - 1 \times 10^{-6}$, the risk is considered as unacceptable according to USEPA, while values below 1×10^{-6} are not considered to pose significant health effects.

3. Results and discussion

3.1. Concentrations and spatial distribution of PTEs

The statistical description of the metals found in the research area is presented in Table 1. The mean metal concentration of the total settled dust (average of *roof and windows concentration*) ranked in the order Al (7.3 %) > Fe (4.1 %) > S (0.6 %) > Ti (0.5 %) > Cu (0.2 %) > Zn (2352.10 mg kg^{-1}) > As (197.76 mg kg^{-1}) > V (131.38 mg kg^{-1}) > Pb (101.86 mg kg^{-1}) > Mo (78.97 mg kg^{-1}) > Cr (42.03 mg kg^{-1}) > Ni (16.24 mg kg^{-1}) > Co (14.45 mg kg^{-1}) > Sb (12.08 mg kg^{-1}) > Cd (2.60 mg kg^{-1}) > Ag (2.40 mg kg^{-1}). Table S3 shows the metal average concentrations in dust obtained from the three surfaces under study (roofs, windows, and soils). All soil samples (17) presented values for Sb below the detection limit (BDL), while Cd and Mo presented 10 and 9 samples BDL.

In general, the concentration of metals in the dust collected from roofs was higher than for windows: 2.2 times higher for Zn, 1.8 for Mo, 1.5 for Cu, 1.4 for Ag, As, and Sb, 1.3 for Pb, 1.1 for Cd, Cr, and Co, 1.0 for Ni, Al, S, Fe, and V, and 0.9 for Ti; and for soils: three times lower than roofs and two times lower than windows. The biggest differences between roof and soils were found for Zn, Mo, Cu, As, and Pb, with concentrations 15, 6, 4, 3, and 2.9 times higher in roof samples (Table S1). Half of the metals under study (Ag, As, Cu, Cd, Mo, S, Sb, and Pb) showed their maximum concentrations in roofs from the villages of Lasana and Cupo (NE of the Talabre tailing dam). Pb concentrations were also close to the maximum at Caspana and Conchi Viejo (to the east and north of Talabre, respectively).

The Coefficient of Variability (CV) was calculated to compare the variability of the element concentration from the total settled dust collected in all sampling sites (Table 1). Zn and Mo showed very high variability with CVs of 141% and 101%, respectively, while Ag, Sb, Cu, As, S, Cd, and Pb showed high variability with CV values between 89% and 62%. These elements mentioned would have the highest possibility of being influenced by specific sources in the area, such as anthropogenic activities. On the other hand, the CV values of Cr and Co (moderate variability) and Ti, V, Fe, Ni, and Al (low variability), indicate that its contents were almost constant across Alto El Loa, suggesting low anthropogenic contribution (Table 1). Highly skewed coefficients were found for Co, Cr, V, Zn, Mo, Ag, S, As, Sb, Ti and Ni, indicating asymmetrical distributions. The skewed coefficients of Fe, Cd and Cu were considered moderately skewed, while Pb and Al, symmetrical. All metals showed kurtosis greater than zero except for Cu, Al, Cd and Pb.

The large variation of the concentration of As, Sb, Zn, Pb Cu, and Mo within Alto El Loa villages shows an inhomogeneity in the region. Mining operations, and mainly the emission from the Talabre tailing dam, might be impacting some of the villages in Alto El Loa. Maximum concentrations were found in Lasana (~13 km from Talabre) and Cupo (~50 km from Talabre), indicating that these villages might be the most exposed due to meteorological factors such wind patterns that determine the transport of pollutants over long distances (Fig. 1). However, we suspect that high Pb concentrations in Conchi Viejo could be associated with the large vehicle fleet from the El Abra mining site, approximately 5 km away from the village. Additionally, the elevated Pb concentrations in Caspana could be due to the use of diesel-powered generators.

The vertical distribution of the concentrations (roofs > windows > soil, 3:2:1) suggested that the dust settling on the roof is less influenced by soil and site-specific conditions, and could be an indicator of potential atmospheric transport. In this sense, roofs may be a good surface for sampling since the signal from local conditions seems to be low. The windows, on the other hand, showed concentrations that could be influenced by both the materials transported from within the community (e.g., soils) and from distant sources (e.g., mining operations). The concentrations of both outdoor surfaces could always enter the indoor environment (Moya and Phillips, 2014; Ibanez et al., 2010; Madany et al., 1994), generating a greater risk for the health of the residents.

3.2. Correlations between PTEs in dust samples and identification of potential sources

The correlation coefficients and statistical significance between all pairs of elements are presented in Table S4 in the supplemental information. Positive and significant ($p \leq 0.001$) correlations were observed between Cu and Ag, Mo, and As with coefficients ranging between 0.82 and 0.96, suggesting a common source. Positive and significant correlation coefficients were also found between As-Cd (0.81) and As-Sb (0.92) (Fig. 2); while Fe showed strong positive and significant correlations with V and Al and negative correlation with As, Cd, and Sb (Fig. 2).

Four principal components (factor 1, factor 2, factor 3, and factor 4) with eigenvalues > 1 were extracted from the PCA analysis (Table S5). These four factors explained 84% of the overall variance, with 43% for factor 1, 24% for factor 2, 8% for factor 3, and 9% for factor 4. Factor 1 has strong positive loading for Cu, As, Cd, Sb, Ag, and Mo, moderate positive loading for Pb and S (the same metals that were seen to have the highest CVs), and weak positive loading for Zn and Cr. Factor 2 has strong positive loading for Fe, V, and Ti, moderate positive loading for Ni and Al, and weak positive loading for Cr. Factor 3 has strong positive loading for Co and weak positive loading for Ni. Factor 4 has moderate positive loading for Zn and Al. The principal component 1 which is the biggest contribution of variability is likely from anthropogenic activities including mining and metal processing and like the CV suggests that Cu, As, Cd, Sb, Ag, and Mo vary significantly between villages. Fig. 3 presents a visual representation of the first two components (PC1 and PC2), their elements and their contributions.

The relationship observed between As, Cd, Sb, Cu, Mo, Ag, and Pb in Factor 1 of Principal Component Analysis and the high and statistically significant correlation coefficients between them suggests they may have resulted from the emission of mining activities through the process of extraction (Cu-Mo) and high-temperature processes and the re-suspension of the Talabre tailing material (As-Cd-Sb-Ag-Mo

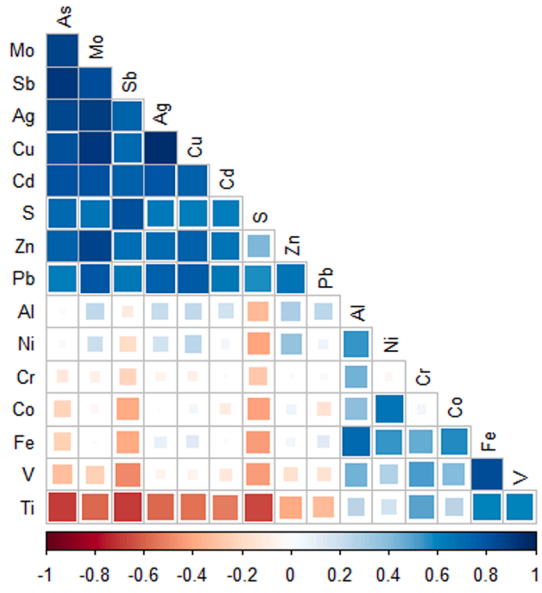

Fig. 2. Correlation matrix showing the covariance between metals for all dust samples collected from Alto El Loa. Each cell shows the correlation between two variables, blue indicates a positive correlation coefficient and red indicates a negative correlation coefficient (or an inverse correlation). The statistical significance is represented by the size and color intensity of the cell. Fully colored cells indicate high statistical significance. Note the high degree of correlation between As, Cd, Sb, Cu, Mo, Ag, S, Zn and Pb.

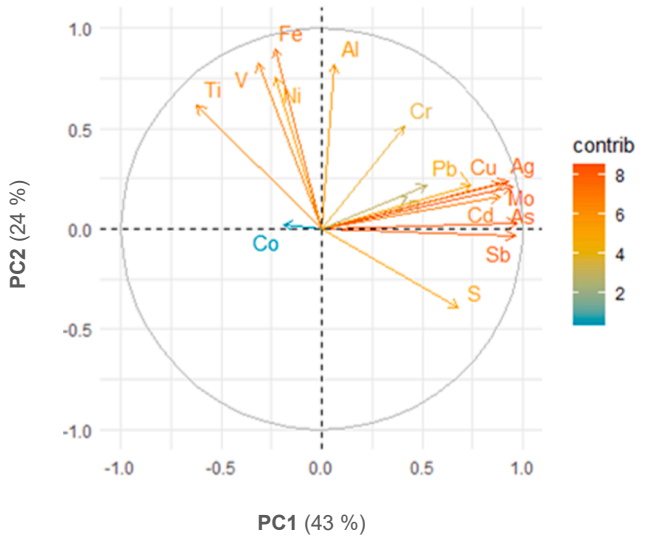

Fig. 3. Biplot for metal concentrations measured in dust samples collected from Alto El Loa. This plot is a visual representation of the first two components (PC1 and PC2). The *x*-axis represents the PC1 explaining 43% of the total variance, and the *y*-axis represents the PC2 explaining 24% of the total variance. The colors of the elements represent the element's contribution to the respective component. Both PC1 and PC2 explain 67% of the total variance.

$r = 0.97–0.90$). The association of these elements to mining emissions and, in particular, to the inadequate management of mine tailings has been reported previously in Cerro de Pasco mining complex in Perú (Molloy et al., 2020), Krugersdorp, South Africa (Ngole-Jeme and Frantke, 2017), and in the Rosh Pinah area, Namibia (Kříbek et al., 2014). Factor 2 (Fe, V, and Ti) and Factor 3 (Co and Ni) are metals characterized by natural emissions, such as rock weathering. Factor 4 (Zn and Al) could be influenced by the roof material "*Aluzinc*", commonly used in the study area, and which composition contains high percentages of Zn (43%), Al (55%), and Si (2%).

A few studies have evaluated the influence of the El Tatio geothermal field and the drainage of its water into the Salado River - a tributary of the Loa basin - for its important contribution of As (Romero et al., 2003) (Fig. 1c). Furthermore, these studies have suggested that El Tatio is the primary source of As in Alto El Loa, while copper mining could be a secondary contributor. Although the present study does not ignore the relevance of El Tatio as a source of As in the El Loa basin, it suggests that the mining activity, and specially the resuspension of dust enriched in metals from the Talabre tailing dam, may have a significant impact on increasing the concentration levels of As and other metals in some of the villages of Alto El Loa. Principal component analysis calculated by Romero et al. (2003) of concentrations obtained from water and sediment samples in the Loa basin suggests that As (with a mean value of 1400 ug/l, or 1.4 mg kg^{-1}) is associated with high concentrations of B and Li, the primary metals found in El Tatio. However, the concentrations of As found in the present study show a strong association with Cu, Sb, and Cd (Fig. 2 and Fig. 3), metals present in high concentration in the sediments of Talabre.

While emissions from the Chuquicamata smelter, inaugurated in 1952, were regulated in 1991 through the control of air emissions of particulate matter (PM), sulfur dioxide (SO_2), arsenic (As), and mercury (Hg) (MINMINERIA, 1991), the Talabre tailings deposit does not have measures to regulate emissions of dust rich in PTEs. In fact, through the NDWI analysis, it was possible to identify that, on average, >60% of the total area is made up of dry surface material (or dry tailings) and would be available for resuspension (Fig. 4). Climate factors such as low water cover, low rainfall, high evaporation, and strong winds could enhance the resuspension and transport of PET from Talabre to the villages in the area (Csavina et al., 2014).

3.3. Transport patterns

The NAME dispersion model was run every 3 h (for the air passing over the surface of Talabre between the 3-hour blocks of 00:00–03:00, 03:00–06:00, …., and 21:00–00:00 every day). Local time is UTC- 3 (except between April and August when it was UTC-4). The NAME runs were done in UTC but the accumulated results showing diurnal cycles were converted to local time. The video in the appendix (V1) collates all these runs, to show the variability and the patterns of the extent of Talabre's influence during 2020. The air often passes over all the villages and other times it follows a narrower and direct route towards Cupo, by-passing the villages in the north. The pattern also varies between seasons, with a broader, more dispersed footprint in winter (May to November) than in the summer. Fig. 5 shows two typical footprints found during the daytime (in January) and nighttime (in September), displaying the typical westerly influence during the day, when the dust from the mine could be transported to the villages and the reverse in wind direction, when easterly nighttime winds would mean that there is unlikely to be a transport from the direction of the mine towards the villages.

The four closest grid boxes ($0.25° \times 0.25°$) around each village were selected so that a regional analysis technique could detect for each 3 hourly footprint what % contribution of the total geographical coverage of the 9 h footprint each village received (Fleming et al., 2012). The results from this analysis were plotted in the summary diurnal cycle for the whole of 2020 in Fig. 6a, showing how between 9:00 and 18:00 local time (GMT-3) all villages received more air from over Talabre (westerly winds). The data has been normalized to show relative contributions for each village. In Fig. 6b, the relative contribution of air passing over Talabre that each village receives has a seasonal influence, with for example Caspana having a greater contribution of air from Talabre in winter and Cupo a greater contribution in summer. Each village receives more air from Talabre during the daytime, but some villages are affected more strongly in certain seasons.

Since we are looking objectively at air mass transport in general and not modelling the behaviour of suspended particles, further research is needed to quantify the flux of atmospheric PM depositing in local villages. Sometimes the air masses could pass over a village and deposit all the dust but other times the dust could remain suspended and be deposited many km away from the source. Molloy et al. (2020) suggests that due to the dryness of the area and the strong winds the area receives, dust particles could travel up to 50 km.

3.4. Pollution indexes

The calculated geo-accumulation index (I_{geo}) values of toxic metals in Alto El Loa are presented in Fig. 7. The mean values of I_{geo} increased in the following order: Ag (0.18) < Cd (0.85) < Mo (7.96) < Pb (9.46) < As (11.20) < Cu (16.72). In almost all samples under study, the I_{geo} values for Cu, As, Cr, Pb, and Mo far exceeded the lower limit of category 6 ($I_{geo} > 5$) or "Extremely contaminated" with ranges between 14.58 and 18.69, 9.92–12.99, 7.73–10.87, and 4.79–10.87, respectively. Cd and Ag values range from "Not polluted" (Category 0) to "Moderately to heavily polluted" (Category 3). The village with the highest I_{geo} values in the study area was Lasana, followed by Cupo (for As and Ag) and Conchi Viejo (for Cu and Mo). On the other hand, the lowest I_{geo} for As, Cu and Ag were found in Toconce and Caspana (the villages directly east and farthest away from Talabre), while Pb has the lowest I_{geo} in Taira, the northernmost village.

The calculated Enrichment Factor (EF) values of toxic metals in Alto El Loa are presented in Fig. 8. The mean values of EF increased in the following order: Cd (1.03) > Ag (1.18) > Pb (3.85) > As (4.51) > Mo (4.65) > Cu (12.91). Almost all samples analysed for Cu and As show enrichment factors above background concentration (EF > 1.5), ranging between 2.00 and 37.00 and 1.44 and 12.73, respectively. The mean EF of Lasana (28.12) reflects very high enrichment, while Cupo (18.50) and

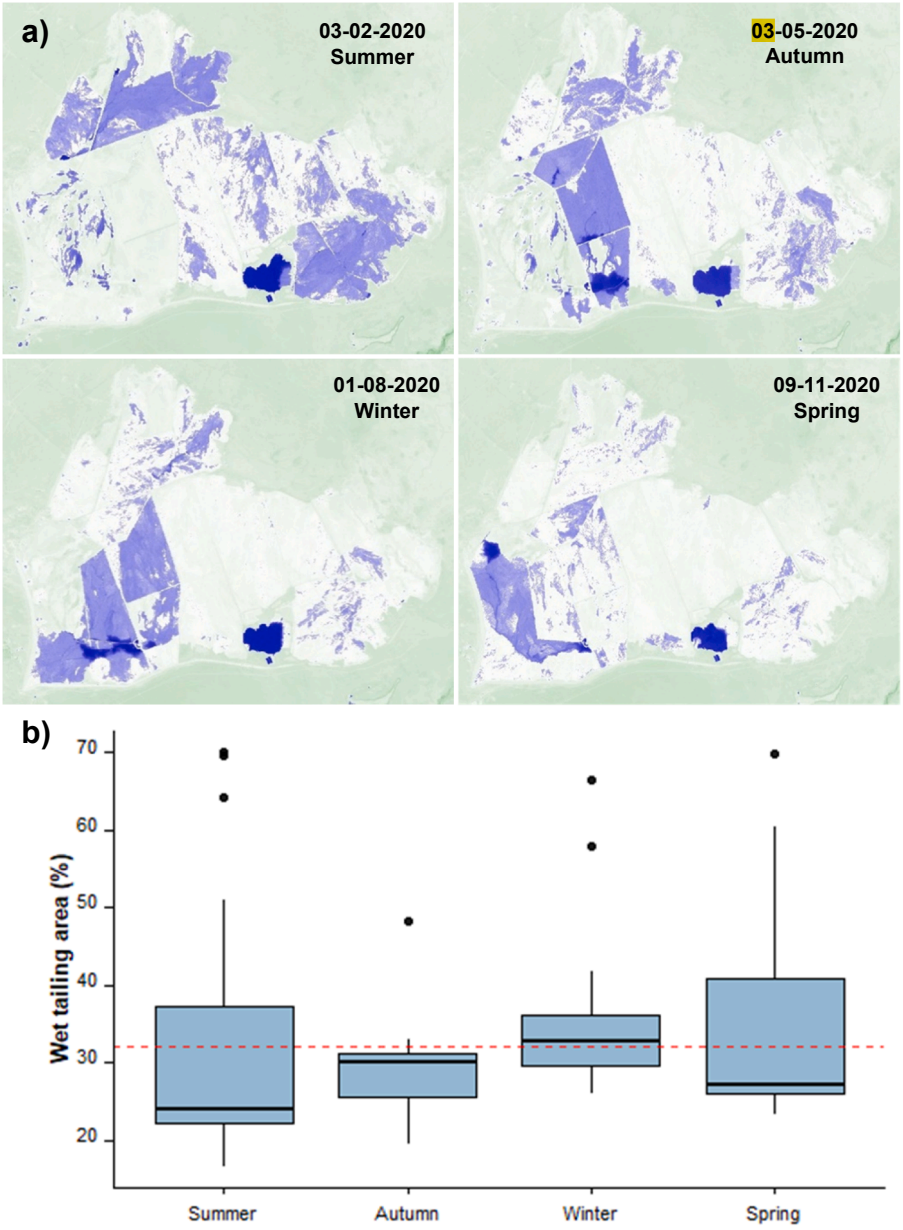

Fig. 4. a) Variation of water content in the Talabre tailing dam viewed by the normalized difference water index (NDWI). This index combines infrared and visible bands, where dark blue represents water, light blue presence of moisture, and light green the absence of water. Maps were obtained from *Sentinel Hub Eo Browser Playground* (see: https://apps.sentinel-hub.com) **b)** Temporal variation of the wet tailing (Threshold > 0.015) in Talabre between 2018 and 2020 viewed by the NDWI. The red dotted line indicates the average wet tailings area for the study period. During the period evaluated, the area of Talabre was 66.5 km^2. To see its size and position relative to the study area, see Fig. 1c.

Conchi (17.14) are at the upper limit of significant enrichment. The highest EFs for As in Lasana and Cupo indicate significant enrichment, while the rest of the Alto El Loa villages show moderate enrichment (2.38 – 4.48). For both metals, the lowest EF values were found in Caspana and Toconce. Lasana and Cupo also show significant enrichments for Mo, with averages of 10.93 and 6.64, respectively, while the rest of the communities show moderate enrichment, except for Toconce, which shows depletion to minimal enrichment. Cd and Ag are less enriched in Alto El Loa than the beforementioned metals, with EFs ranging between 1.52 and 0.36 for Cd and between 4.21 and 0.26 for Ag. However, the highest enrichments for Cd and Ag, as well as for Cu, As, and Mo, are also found at Lasana and Cupo. Lasana and Cupo showed a higher variability for both I_{geo} and EF between the samples, but in general higher levels than in the other villages for most metals. Finally, all villages in Alto El Loa showed enrichment factors > 0 for Pb, indicating an anthropogenic contribution.

The results obtained through the calculation of pollution indices with these regional average concentrations should be considered with caution and only as a preliminary approximation until a complete study of the background levels of metals is carried out locally. However, the metals that were highlighted to show greater prominence and accumulation within villages were similar to those found in the variability analysis and in the principal component analysis (As, Cu, Pb, Mo, Ag and Cd and Cr to a lesser extent).

3.5. Health risk assessment

The calculated hazard quotient (HQ) by ingestion of potentially toxic elements (PTEs) in Alto El Loa villages is illustrated in Fig. 9. The spatial distribution of HQ in Alto El Loa presents a similar pattern in almost all elements evaluated, suggesting a higher potential non-carcinogenic risk to children from potential dust ingestion in Lasana and Cupo. This is consistent with the contamination levels (I_{geo}, Fig. 7) and enrichment (EF, Fig. 8) presented and discussed in previous sections.

Arsenic is the PTE with the highest potential non-carcinogenic risk in Alto El Loa, where all communities present a risk above the accepted level (HQ ≤ 1). While the average of Alto El Loa communities exceeds up to 7.08 times the accepted levels, some samples in Lasana and Cupo

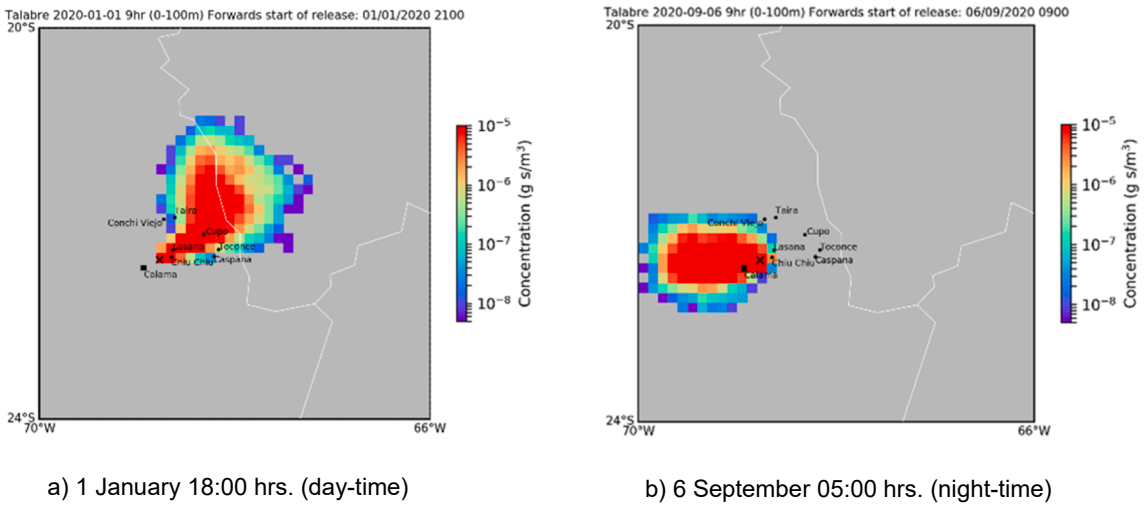

Fig. 5. An example of 3 hourly footprints of where the air from Talabre travels during a period of 9 h at surface (0–100 m levels). **a)** On the 1st of January (21:00 UTC) (1st January 18:00 local time) the air passed over Lasana and Cupo, avoiding the more northerly villages like Conchi Viejo and Taira. **b)** On the 6th of September at 09:00 UTC (05:00 local time) one can see when easterly night-time winds blow, Talabre wouldńt affect the villages. The air frequently travels into Bolivia within < 9 h and could deposit dust from the tailings on any of these surfaces it has passed over. The colors in the legend are logarithmic, with red showing in the areas where the air spends most time.

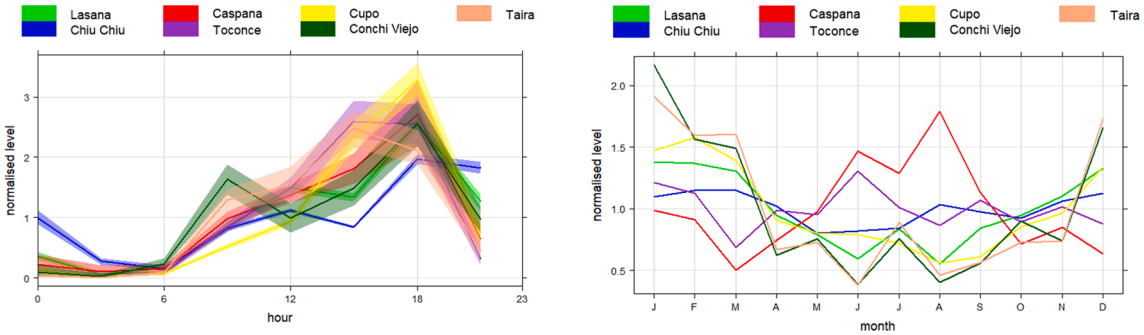

Fig. 6. **a)** Relative contribution of air masses that pass over Talabre arriving at each village according to time of day (showing the standard deviation over the whole year). **b)** Relative contribution of air masses from Talabre on each village (shown as monthly averages).

exceeded them by up to 20 times. Although it is known that this region is geologically enriched by arsenic (Romero et al. 2003), the fact that the communities of Lasana and Cupo present an average risk higher than the others suggests an anthropogenic influence and, concerning the transport models presented in previous sections, this difference could be better explained by the transport of As-rich dust from the Talabre tailings dam (Fig. 4). After ingestion, at least 90% of inorganic arsenic is absorbed via the gastrointestinal route and distributed through the blood to different organs such as the liver, kidneys, lungs, and bladder (Watanabe and Hirano, 2013). Although health effects cannot be determined through this study, possible health effects associated with arsenic ingestion include cardiovascular and peripheral vascular diseases, developmental abnormalities, neurological and neurobehavioral disorders, diabetes, portal fibrosis, hematological disorders, and multiple cancers such as skin, lung, liver, urinary bladder, kidney, and colon cancers (Tchounwou et al., 2003). Therefore, studies and public policy measures to mitigate the potential adverse effects on children's health in Alto El Loa should be undertaken urgently.

Although Sb, Cd, Mo, and Ag are PTEs that we have associated in this study with emissions from the Talabre tailings, our results here suggest that the communities of Alto El Loa are not yet experiencing a health risk from ingestion of these elements. However, increased emissions - due to projected increases in production (Elshkaki et al., 2016) - could increase the risk, especially for Sb, which is close to acceptable limits in some villages (Fig. 9). On the other hand, almost all dust samples taken in the communities of Lasana, Conchi Viejo, and Cupo exceeded the accepted limits for Cu. In this case, Conchi Viejo joins Lasana and Cupo (which, as already mentioned, could be affected by the transport of dust from Talabre) since the copper extraction site of the El Abra mining company is located within the community area (Fig. 1). Finally, the ingestion of dust by children in the communities of Lasana, Conchi Viejo, Cupo, and Caspana could pose a potential non-carcinogenic risk to them by Pb, given that their levels are above the accepted limits. As we have mentioned in previous sections, the influence of the passage and permanence of vehicles in Conchi Viejo (due to the proximity to the El Abra mining company) and the use of fossil fuels for energy supply in the town of Caspana could be increasing the risk in these communities.

When considering the addition of more than one toxic element through the Hazard Index (HI) (Fig. 9), all villages had exceeded the safe threshold (HI ≤ 1), thus indicating a potential non-carcinogenic effect of ingestion of settled dust. The values of HI indices were the highest in Lasana (HI between 12.97 and 25.28), followed by Cupo (HI between 5.02 and 24.78), Conchi (HI between 4.30 and 12.35), Chiu Chiu (HI between 4.34 and 12.89), Caspana (HI between 3.39 and 8.72), Taira (HI between 3.61 and 7.20), and Toconce (HI between 2.85 and 9.35).

For carcinogenic risk due to As ingestion (Fig. 10), the ranking of *CR* in the seven villages of Alto El Loa was Lasana ($6.42x10^{-03}$) > Cupo ($5.43x10^{-03}$) > Chiu Chiu ($2.84x10^{-03}$) > Conchi Viejo ($2.51x10^{-03}$) > Toconce ($1.93x10^{-03}$) > Taira ($1.92x10^{-03}$) > Caspana ($1.77x10^{-03}$), with all samples in Alto El Loa exceeding the upper limit

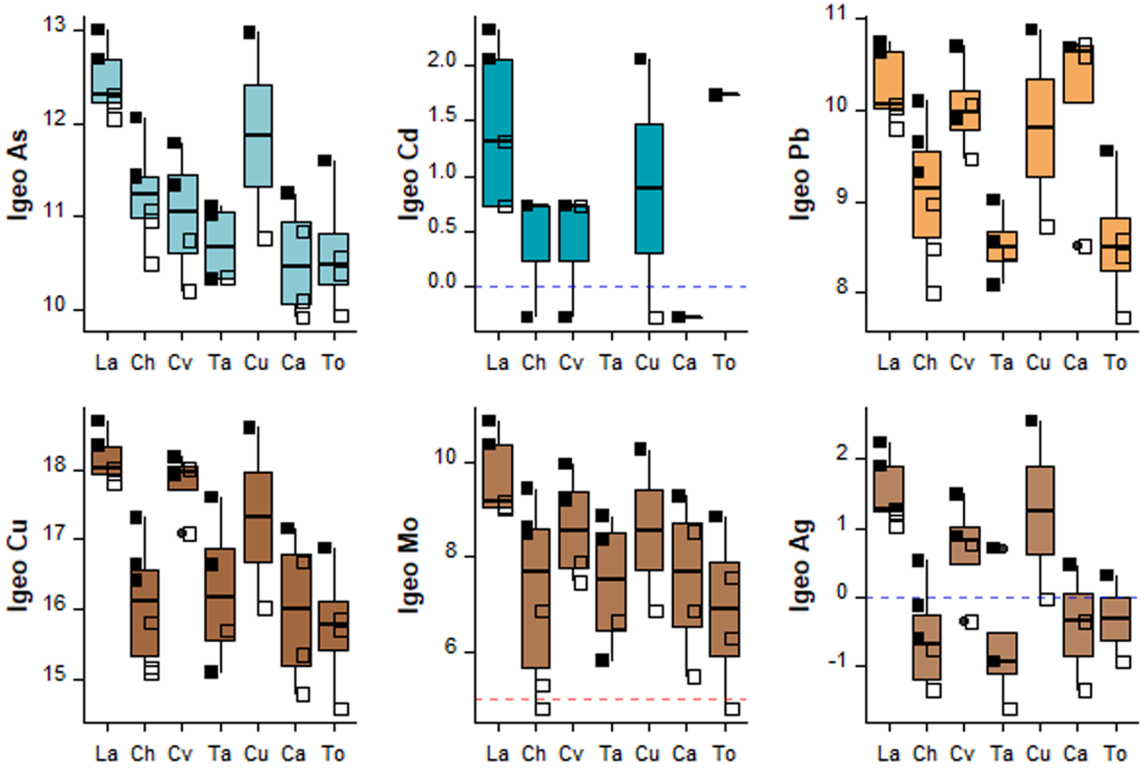

Fig. 7. Geoaccumulation index (I_{geo}) of the Indigenous Villages in IDA Alto El Loa. Roof samples are presented with black squares, while window samples are presented with white squares. The blue dotted line indicates the upper limit of category 0: Not polluted, while the red dotted line indicates the lower limit of category 6: Extremely polluted. The villages shown in Fig. 1 are Lasana (La), Chiu Chiu (Ch) (close-by to the east), Conchi Viejo (Cv), Taire (Ta) (to the north), and Cupo (Cu), Caspana (Ca) and Toconce (To) (to the east).

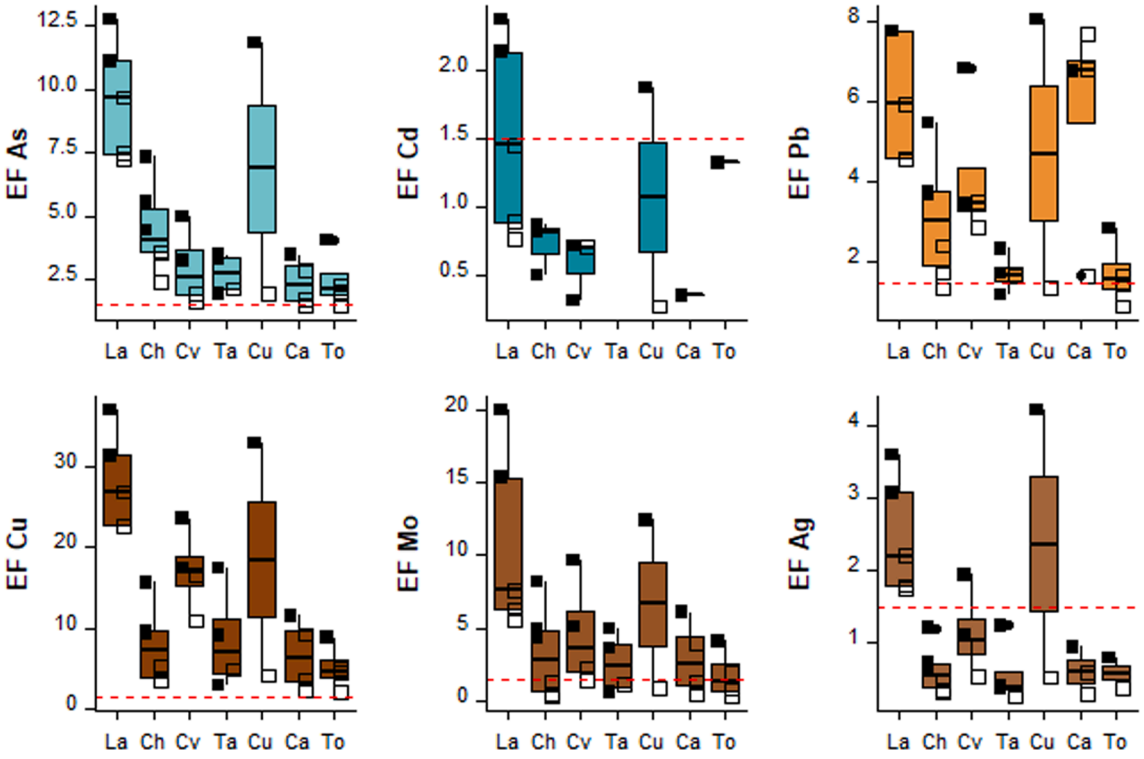

Fig. 8. Enrichment Factor (EF) of the Indigenous Villages in IDA Alto El Loa. Roof samples are presented with black squares, while window samples are presented with white squares. The red dotted line (1.0 on the y-axis) indicates the boundary between natural contribution (<1.5) and anthropogenic effect (>1.5). The villages shown in Fig. 1 are Lasana (La), Chiu Chiu (Ch) (close-by to the east), Conchi Viejo (Cv), Taire (Ta) (to the north), and Cupo (Cu), Caspana (Ca) and Toconce (To) (to the east).

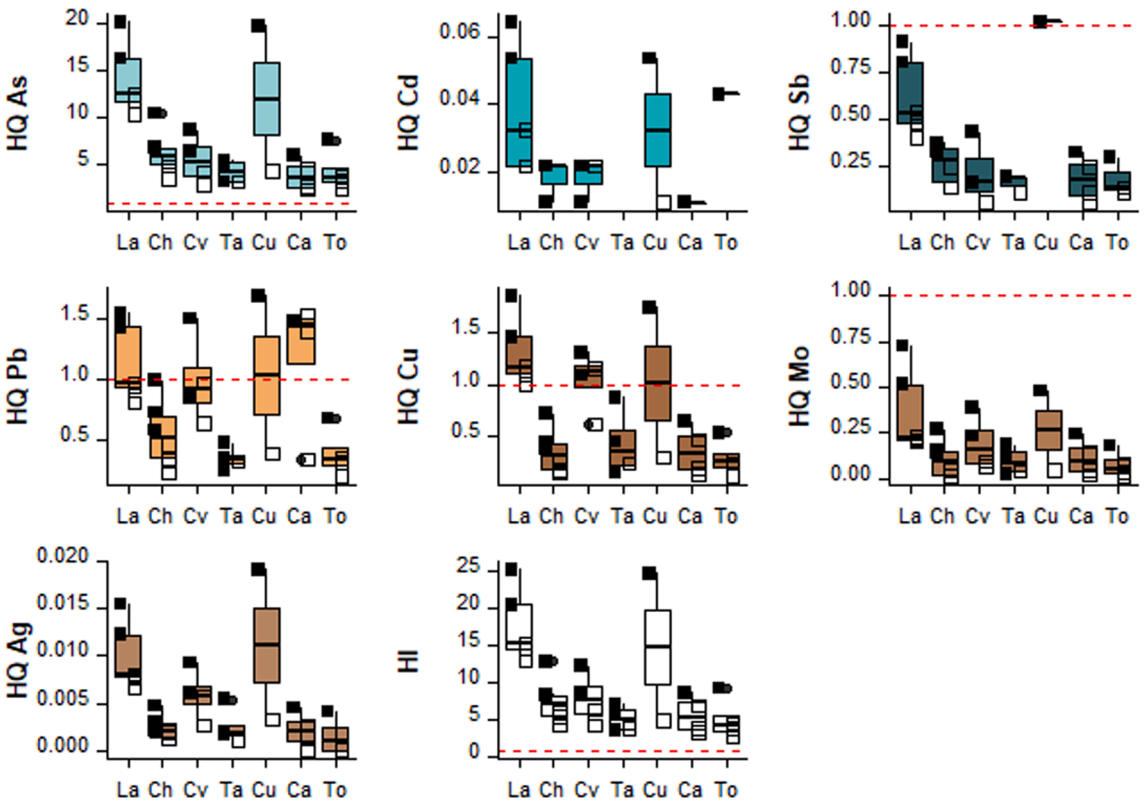

Fig. 9. HQ for each metal and total HI for Ingestion in Alto El Loa. The red dotted line indicates the accepted level limit (HQ ≤ 1). Roof samples are presented with black squares, while window samples are presented with white squares. The villages shown in Fig. 1 are Lasana (La), Chiu Chiu (Ch) (close-by to the east), Conchi Viejo (Cv), Taire (Ta) (to the north), and Cupo (Cu), Caspana (Ca) and Toconce (To) (to the east).

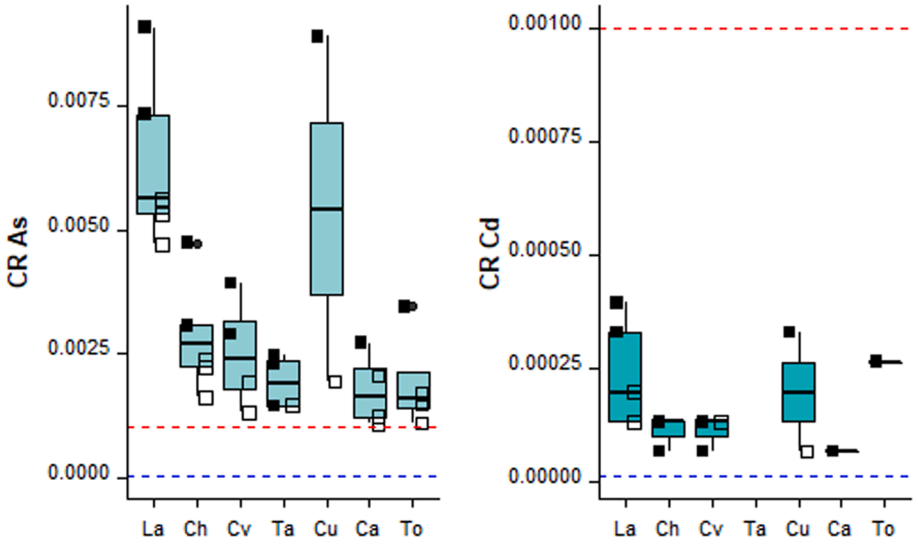

Fig. 10. CR for As and Cd for Children in Alto El Loa. The blue dotted line (10^{-06}, lower limit) and the red dotted line (10^{-04}, upper limit) indicate acceptable ranges. Roof samples are presented with black squares, while window samples are presented with white squares. The villages shown in Fig. 1 are Lasana (La), Chiu Chiu (Ch) (close-by to the east), Conchi Viejo (Cv), Taire (Ta) (to the north), and Cupo (Cu), Caspana (Ca) and Toconce (To) (to the east).

of the accepted range (10^{-04}), showing a high carcinogenic risk. With values up to 9.09 and 8.91 times above the upper limit of the accepted range, Lasana and Cupo, respectively, have CRs 1.97 and 1.67 times higher than the Alto El Loa average and 3.49 and 2.95 times higher than the average of the communities with the lowest CR in the study area (Caspana y Taira). On the other hand, the CR values for Cd are within the accepted ranges (Fig. 9), with no carcinogenic risk for children in Alto El Loa through potential Cd ingestion.

4. Conclusions

Our study suggests that the variations in As, Sb, Cd, Cu, Mo, Ag, Pb, and S concentrations in outdoor settled dust in the Alto El Loa villages can be explained by emissions from mining activities. The Talabre tailing dam -adjacent to Indigenous villages- can be an important source of dust containing high concentrations of potentially toxic elements and the predominant winds could easily transport this to neighbouring

villages. Our results indeed indicate that wind direction and intensity play a pivotal role in the transport of dust particles, particularly during the daytime, but also seasonally.

The highest concentrations, as well as the highest variability in the trace metals were found in the villages of Lasana and Cupo, to the northeast of the Talabre tailings and downwind of the mine during the daytime hours. Zn, Mo, Ag, Sb, Cu, As, S, Cd and Pb were the metals that appeared to vary most strongly between the villages and between types of dust samples, with the dust on the roofs containing more than that on the windowsills and more than that in the soil. Lasana and Cupo had higher geoaccumulation indexes, trace metal enrichment factors, hazard quotients (for individual metals), hazard indexes (for combined metals) and carcinogenic risks than the other villages.

The communities of Alto El Loa experience a pollution burden that has affected the environmental health and potentially increased non-carcinogenic and carcinogenic risks. In a geologically diverse geography like Chile, geochemical background studies on a local scale are needed for a better evaluation of environmental and health risks of potentially toxic elements to communities.

In this sense, the Talabre tailings dam represents an underestimated local socio-environmental hazard, the management of which should rely on spatio-temporal planning for envisioning a sustainable future either for indigenous communities or ecosystems. This is especially true when considering the increased copper demand in the coming decades, a scenario that calls for the need for challenging actions for achieving SDGs in certain critical areas close to mining complexes.

CRediT authorship contribution statement

Nicolás C. Zanetta-Colombo: Conceptualization, Investigation, Formal analysis, Visualization, Writing – original draft. **Zoë L. Fleming:** Investigation, Writing – original draft, Funding acquisition. **Eugenia M. Gayo:** Conceptualization, Writing – review & editing. **Carlos A. Manzano:** Investigation, Writing – original draft, Funding acquisition. **Marios Panagi:** Formal analysis, Visualization. **Jorge Valdés:** Writing – review & editing. **Alexander Siegmund:** Writing – review & editing, Resources.

Declaration of Competing Interest

The authors declare that they have no known competing financial interests or personal relationships that could have appeared to influence the work reported in this paper.

Data availability

Data will be made available on request.

Acknowledgements

The authors thank the indigenous communities of Alto El Loa who made this work possible. Nicolás Zanetta-Colombo is especially grateful to the Deutschen Akademischen Austauschdienstes (DAAD) who have provided funding for the development of his Ph.D. thesis (Funding program "Research Grants – Doctoral Programs in Germany, 2020-21"). Special thanks to the UK National Environmental Research Council (NERC) Jasmin supercomputer at STFC for running the NAME model and to the UK Met Office for the use of the Unified Model (UM) Met data and the use of the NAME model. We would also like to thank The Center for Climate and Resilience research (CR)2 (ANID/FONDAP/15110009) and Upwell (ANID-MillenniumScience Initiative Program – NCN19_153) for supporting this research. Funding for this research was provided by FONDECYT grant #11180151, FONDECYT grant #1221951, FONDEQUIP Mayor grant EQY200021, from the Chilean Agency for Research and Development (ANID).

Appendix A. Supplementary material

Supplementary data to this article can be found online at https://doi.org/10.1016/j.envint.2022.107490.

References

Amato, F., Pandolfi, M., Viana, M., Querol, X., Alastuey, A., Moreno, T., 2009. Spatial and chemical patterns of PM10 in road dust deposited in urban environment. Atmos. Environ. 43 (9), 1650–1659.

Barbieri, M., 2016. The Importance of Enrichment Factor (EF) and Geoaccumulation Index (Igeo) to Evaluate the Soil Contamination. J. Geol. Geophys. 5 (1) https://doi.org/10.4172/2381-8719.1000237.

Brown, A., Milton, S., Cullen, M., Golding, B., Mitchell, J., Shelly, A., 2012. Unified modeling and prediction of weather and climate: a 25-year journey. Bull. Am. Meteorol. Soc. 93 (12), 1865–1877. https://doi.org/10.1175/BAMS-D-12-00018.1.

Calderón-Seguel, M., Prieto, M., Meseguer-Ruiz, O., Viñales, F., Hidalgo, P., Esper, E., 2021. Mining, urban growth, and agrarian changes in the Atacama Desert: the case of the Calama Oasis in Northern Chile. Land 10 (11), 1262.

Cameron, E.M., Leybourne, M.I., Palacios, C., Reich, M., 2008. Economic Geology Models 1. Geochemical Exploration and Metallogenic Studies, Northern Chile. Geoscience Canada. https://journals.lib.unb.ca/index.php/GC/article/view/11269.

Cao, S., Duan, X., Zhao, X., Wang, B., Ma, J., Fan, D., Sun, C., He, B., Wei, F., Jiang, G., 2015. Health risk assessment of various metal(loid)s via multiple exposure pathways on children living near a typical lead-acid battery plant, China. Environ. Pollut. 200, 16–23. https://doi.org/10.1016/j.envpol.2015.02.010.

Carrasco, A., 2015. Jobs and kindness: W.E. Rudolph's role in the shaping of perceptions of mining company-indigenous community relations in the Atacama Desert, Chile. Extractive Indust. Soc. 2 (2), 352–359. https://doi.org/10.1016/j.exis.2014.11.008.

CENMA, 2014. Diagnostico regional de suelos abandonados con potencial presencia de contaminantes, pp. 1–110 [Informe final].

Cerda, M., Evangelista, H., Valdés, J., Siffedine, A., Boucher, H., Nogueira, J., Nepomuceno, A., Ortlieb, L., 2019. A new 20th century lake sedimentary record from the Atacama Desert/Chile reveals persistent PDO (Pacific Decadal Oscillation) impact. J. S. Am. Earth Sci. 95, 102302 https://doi.org/10.1016/j.jsames.2019.102302.

Chui Betancur, H.N., Acosta Najarro, D.R., Olivera de Lescano, P.O., 2016. Characterization of sediments deposited on the roof of houses near the plant cesur sa in Caracoto district, Peru. Revista Boliviana de Química 33 (2), 43–49.

Csavina, J., Field, J., Taylor, M.P., Gao, S., Landázuri, A., Betterton, E.A., Sáez, A.E., 2012. A review on the importance of metals and metalloids in atmospheric dust and aerosol from mining operations. Sci. Total Environ. 433, 58–73. https://doi.org/10.1016/j.scitotenv.2012.06.013.

Csavina, J., Field, J., Félix, O., Corral-Avitia, A.Y., Sáez, A.E., Betterton, E.A., 2014. Effect of wind speed and relative humidity on atmospheric dust concentrations in semi-arid climates. Sci. Total Environ. 487, 82–90.

De Gregori, I., Fuentes, E., Rojas, M., Pinochet, H., Potin-Gautier, M., 2003. Monitoring of copper, arsenic and antimony levels in agricultural soils impacted and non-impacted by mining activities, from three regions in Chile. J. Environ. Monit.: JEM 5 (2), 287–295. https://doi.org/10.1039/b211469k.

Dietz, T., Whitley, C.T., 2018. Environmentalism, norms, and identity. Proc. Natl. Acad. Sci. USA 115 (49), 12334–12336.

Doyi, I.N.Y., Isley, C.F., Soltani, N.S., Taylor, M.P., 2019. Human exposure and risk associated with trace element concentrations in indoor dust from Australian homes. Environ. Int. 133, 105125.

Eichler, A., Gramlich, G., Kellerhals, T., Tobler, L., Rehren, T., Schwikowski, M., 2017. Ice-core evidence of earliest extensive copper metallurgy in the Andes 2700 years ago. Sci. Rep. 7 (1), 41855. https://doi.org/10.1038/srep41855.

Eichler, A., Gramlich, G., Kellerhals, T., Tobler, L., Schwikowski, M., 2015. Pb pollution from leaded gasoline in South America in the context of a 2000-year metallurgical history. Sci. Adv. 1 (2), e1400196 https://doi.org/10.1126/sciadv.1400196.

Elshkaki, A., Graedel, T.E., Ciacci, L., Reck, B.K., 2016. Copper demand, supply, and associated energy use to 2050. Global Environ. Change 39, 305–315. https://doi.org/10.1016/j.gloenvcha.2016.06.006.

Fleming, Zoë L., Monks, Paul S., Manning, Alistair J., 2012. Untangling the influence of air-mass history in interpreting observed atmospheric composition. Atmos. Res. 104, 1–39. https://doi.org/10.1016/j.atmosres.2011.09.009. ISSN 0169-8095.

Förstner, U., Salomons, W., 1980. Trace metal analysis on polluted sediments: Part I: Assessment of sources and intensities. Environ. Technol. Lett. 1 (11), 494–505. https://doi.org/10.1080/09593338009384006.

Fuller, D.R., 2004. The production of copper in 6th century Chile's chuquicamata mine. JOM 56 (11), 62–66. https://doi.org/10.1007/s11837-004-0256-6.

Gayo, E.M., McRostie, V.B., Campbell, R., Flores, C., Maldonado, A., Uribe-Rodriguez, M., Moreno, P.I., Santoro, C.M., Christie, D.A., Muñoz, A.A., Gallardo, L., 2019. Geohistorical records of the Anthropocene in Chile. Elem. Sci. Anth. 7, 15. https://doi.org/10.1525/elementa.353.

Gohain, M., Deka, P., 2020. Trace metals in indoor dust from a university campus in Northeast India: implication for health risk. Environ. Monit. Assess. 192 (11), 741. https://doi.org/10.1007/s10661-020-08684-6.

González-Rojas, C.H., Leiva-Guzmán, M., Manzano, C.A., Araya, R.T., 2021. Short term air pollution events in the Atacama desert, Chile. J. S. Am. Earth Sci. 105, 103010.

Hao, L., Zhang, Z., Yang, X., 2019. Mine tailing extraction indexes and model using remote-sensing images in southeast Hubei Province. Environ. Earth Sci. 78 (15), 493. https://doi.org/10.1007/s12665-019-8439-1.

Herrera, C., Godfrey, L., Urrutia, J., Custodio, E., Jordan, T., Jódar, J., Delgado, K., Barrenechea, F., 2021. Recharge and residence times of groundwater in hyper arid areas: the confined aquifer of Calama, Loa River Basin, Atacama Desert, Chile. Sci. Total Environ. 752, 141847 https://doi.org/10.1016/j.scitotenv.2020.141847.

Horowitz, A.J., Rinella, F.A., Lamothe, P., Miller, T.L., Edwards, T.K., Roche, R.L., Rickert, D.A., 1990. Variations in suspended sediment and associated trace element concentrations in selected riverine cross sections. Environ. Sci. Technol. 24 (9), 1313–1320. https://doi.org/10.1021/es00079a003.

Hou, S., Zheng, N., Tang, L., Ji, X., Li, Y., Hua, X., 2019. Pollution characteristics, sources, and health risk assessment of human exposure to Cu, Zn, Cd and Pb pollution in urban street dust across China between 2009 and 2018. Environ. Int. 128, 430–437.

Houston, J., 2006. Variability of precipitation in the Atacama Desert: Its causes and hydrological impact. Int. J. Climatol. 26 (15), 2181–2198. https://doi.org/10.1002/joc.1359.

Houston, J., Hartley, A.J., 2003. The central Andean west-slope rainshadow and its potential contribution to the origin of hyper-aridity in the Atacama Desert. Int. J. Climatol. 23 (12), 1453–1464. https://doi.org/10.1002/joc.938.

Huang, M., Zhou, S., Sun, B., Zhao, Q., 2008. Heavy metals in wheat grain: assessment of potential health risk for inhabitants in Kunshan, China. Sci. Total Environ. 405 (1), 54–61. https://doi.org/10.1016/j.scitotenv.2008.07.004.

Ibanez, Y., Le Bot, B., Glorennec, P., 2010. House-dust metal content and bioaccessibility: a review. Eur. J. Mineral. 22 (5), 629–637. https://doi.org/10.1127/0935-1221/2010/0022-2010.

INE, 2018. Instituto Nacional de Estadísticas de Chile. Estimaciones y Proyecciones de la Población de Chile 1992-2050. Santiago, Chile.

Jones, A., Thomson, D., Hort, M., Devenish, B., 2007. The U.K. Met Office's Next-Generation Atmospheric Dispersion Model, NAME III. In: Borrego, C., Norman, A.-L. (Eds.), Air Pollution Modeling and Its Application XVII. Springer, US, pp. 580–589. https://doi.org/10.1007/978-0-387-68854-1_62.

Khan, A., Khan, S., Khan, M.A., Qamar, Z., Waqas, M., 2015. The uptake and bioaccumulation of heavy metals by food plants, their effects on plants nutrients, and associated health risk: a review. Environ. Sci. Pollut. Res. 22 (18), 13772–13799. https://doi.org/10.1007/s11356-015-4881-0.

Kříbek, B., Majer, V., Pašava, J., Kamona, F., Mapani, B., Keder, J., Ettler, V., 2014. Contamination of soils with dust fallout from the tailings dam at the Rosh Pinah area, Namibia: Regional assessment, dust dispersion modeling and environmental consequences. J. Geochem. Explor. 144, 391–408.

Lee, P.-K., Kang, M.-J., Yu, S., Kwon, Y.K., 2020. Assessment of trace metal pollution in roof dusts and soils near a large Zn smelter. Sci. Total Environ. 713, 136536.

Lilic, N., Cvjetic, A., Knezevic, D., Milisavljevic, V., Pantelic, U., 2018. Dust and noise environmental impact assessment and control in Serbian mining practice. Minerals 8 (2), 34.

Malakootian, M., Mohammadi, A., Nasiri, A., et al., 2021. Spatial distribution and correlations among elements in smaller than 75 μm street dust: ecological and probabilistic health risk assessment. Environ. Geochem. Health 43, 567–583.

Madany, I.M., Salim Akhter, M., Al Jowder, O.A., 1994. The correlations between heavy metals in residential indoor dust and outdoor street dust in Bahrain. Environ. Int. 20 (4), 483–492. https://doi.org/10.1016/0160-4120(94)90197-X.

Madrid, E., Gonzalez-Miranda, I., Muñoz, S., Rejas, C., Cardemil, F., Martinez, F., Cortes, J.P., Berasaluce, M., Párraga, M., 2022. Arsenic concentration in topsoil of central Chile is associated with aberrant methylation of P53 gene in human blood cells: A cross-sectional study. Environ. Sci. Pollut. Res. 29 (32), 48250–48259.

Manzano, C.A., Jácome, M., Syn, T., Molina, C., Toro Araya, R., Leiva-Guzmán, M.A., 2021. Local air quality issues and research priorities through the lenses of Chilean experts: an ontological analysis. Integr. Environ. Assess. Manage. 17 (1), 273–281. https://doi.org/10.1002/ieam.4320.

MINMINERIA, 1991. Decreto 185. Reglamenta funcionamiento de establecimientos emisores de anhidrido sulfuroso, material particulado y arsénico en todo el territorio de la republica. Ministerio de Minería. Santiago de Chile. 16.01.1992.

Monjezi, M., Shahriar, K., Dehghani, H., Samimi Namin, F., 2009. Environmental impact assessment of open pit mining in Iran. Environ. Geol. 58 (1), 205–216.

Moya, J., Phillips, L., 2014. A review of soil and dust ingestion studies for children. J. Eposure Sci. Environ. Epidemiol. 24 (6), 545–554. https://doi.org/10.1038/jes.2014.17.

Moya, P.M., Arce, G.J., Leiva, C., Vega, A.S., Gutiérrez, S., Adaros, H., Muñoz, L., Pastén, P.A., Cortés, S., 2019. An integrated study of health, environmental and socioeconomic indicators in a mining-impacted community exposed to metal enrichment. Environ. Geochem. Health 41 (6), 2505–2519.

Molloy, J.B., Rodbell, D.T., Gillikin, D.P., Hollocher, K.T., 2020. Citizen science campaign reveals widespread fallout of contaminated dust from mining activities in the central Peruvian Andes. Geology 48 (7), 678–682. https://doi.org/10.1130/G47096.1.

Mudd, G.M., Roche, C., Northey, S.A., Jowitt, S.M., Gamato, G., 2020. Mining in Papua New Guinea: a complex story of trends, impacts and governance. Sci. Total Environ. 741, 140375.

Müller, G., 1979. Schwermetalle in den Sedimenten des Rheins-Veranderungen seit 1971. Umschau 24, 778–783.

Müller, G., 1981. Die Schwermetallbelstrung der sedimente des Neckar und seiner Nebenflusse: Eine Bestandsaufnahme. ChemikerZeitung 105, 156–164.

Muñoz, A.A., Klock-Barría, K., Sheppard, P.R., Aguilera-Betti, I., Toledo-Guerrero, I., Christie, D.A., Gorena, T., Gallardo, L., González-Reyes, Á., Lara, A., Lambert, F., Gayo, E., Barraza, F., Chávez, R.O., 2019. Multidecadal environmental pollution in a mega-industrial area in central Chile registered by tree rings. Sci. Total Environ. 696, 133915 https://doi.org/10.1016/j.scitotenv.2019.133915.

Muñoz, R.C., Falvey, M.J., Arancibia, M., Astudillo, V.I., Elgueta, J., Ibarra, M., Santana, C., Vásquez, C., 2018. Wind energy exploration over the Atacama Desert: a numerical model-guided observational program. Bull. Am. Meteorol. Soc. 99 (10), 2079–2092. https://doi.org/10.1175/BAMS-D-17-0019.1.

Ngole-Jeme, V.M., Fantke, P., Paz-Ferreiro, J., 2017. Ecological and human health risks associated with abandoned gold mine tailings contaminated soil. PLoS ONE 12 (2), e0172517.

Ossandon, G., Freraut, C.R., Gustafson, L.B., Lindsay, D.D., Zentilli, M., 2001. Geology of the chuquicamata mine: a progress report. Econ. Geol. 96 (2), 249–270.

Palacios, C., Ramírez, L.E., Townley, B., Solari, M., Guerra, N., 2007. The role of the Antofagasta-Calama Lineament in ore deposit deformation in the Andes of northern Chile. Miner. Deposita 42 (3), 301–308. https://doi.org/10.1007/s00126-006-0113-3.

Pandey, P.K., Sharma, R., Roy, M., Pandey, M., 2007. Toxic mine drainage from Asia's biggest copper mine at Malanjkhand, India. Environ. Geochem. Health 29 (3), 237–248.

Pearson, A.R., Schuldt, J.P., Romero-Canyas, R., Ballew, M.T., Larson-Konar, D., 2018. Diverse segments of the US public underestimate the environmental concerns of minority and low-income Americans. Proc. Natl. Acad. Sci. USA 115 (49), 12429–12434.

Fan, P., Lu, X., Yu, B.o., Fan, X., Wang, L., Lei, K., Yang, Y., Zuo, L., Rinklebe, J., 2022. Spatial distribution, risk estimation and source apportionment of potentially toxic metal(loid)s in resuspended megacity street dust. Environ. Int. 160, 107073.

Kurt-Karakus, P.B., 2012. Determination of heavy metals in indoor dust from Istanbul, Turkey: estimation of the health risk. Environ. Int. 50, 47–55.

Pourret, O., Bollinger, J.-C., Hursthouse, A., 2021. Heavy metal: a misused term? Acta Geochim. 40 (3), 466–471. https://doi.org/10.1007/s11631-021-00468-0.

Ramírez, L.E., Palacios, C., Townley, B., Parada, M.A., Sial, A.N., Fernandez-Turiel, J.L., Gimeno, D., Garcia-Valles, M., Lehmann, B., 2006. The Mantos Blancos copper deposit: an upper Jurassic breccia-style hydrothermal system in the Coastal Range of Northern Chile. Miner. Deposita 41 (3), 246. https://doi.org/10.1007/s00126-006-0055-9.

Romero, L., Alonso, H., Campano, P., Fanfani, L., Cidu, R., Dadea, C., Keegan, T., Thornton, I., Farago, M., 2003. Arsenic enrichment in waters and sediments of the Rio Loa (Second Region, Chile). Appl. Geochem. 18 (9), 1399–1416. https://doi.org/10.1016/S0883-2927(03)00059-3.

Romero-Toledo, H., 2019. Extractivismo en Chile: La producción del territorio minero y las luchas del pueblo aimara en el Norte Grande. Colombia Internacional 98, 3–30. https://doi.org/10.7440/colombiaint98.2019.01.

Rout, T.K., Masto, R.E., Ram, L.C., George, J., Padhy, P.K., 2013. Assessment of human health risks from heavy metals in outdoor dust samples in a coal mining area. Environ. Geochem. Health 35 (3), 347–356.

Sall, M.L., Diaw, A.K.D., Gningue-Sall, D., Efremova Aaron, S., Aaron, J.-J., 2020. Toxic heavy metals: Impact on the environment and human health, and treatment with conducting organic polymers, a review. Environ. Sci. Pollut. Res. 27 (24), 29927–29942. https://doi.org/10.1007/s11356-020-09354-3.

Schipper, B.W., Lin, H.-C., Meloni, M.A., Wansleeben, K., Heijungs, R., van der Voet, E., 2018. Estimating global copper demand until 2100 with regression and stock dynamics. Resour. Conserv. Recycl. 132, 28–36. https://doi.org/10.1016/j.resconrec.2018.01.004.

Schwanck, F., Simões, J.C., Handley, M., Mayewski, P.A., Bernardo, R.T., Aquino, F.E., 2016. Anomalously high arsenic concentration in a West Antarctic ice core and its relationship to copper mining in Chile. Atmos. Environ. 125, 257–264. https://doi.org/10.1016/j.atmosenv.2015.11.027.

Shi, T., Wang, Y., 2021. Heavy metals in indoor dust: Spatial distribution, influencing factors, and potential health risks. Sci. Total Environ. 755 (Pt 1), 142367.

Smart, S., 2017. Resistance against mining extractivism in Chile. Crit. Plan. 23 https://doi.org/10.5070/CP8231038128.

Smuda, J., Dold, B., Spangenberg, J.E., Friese, K., Kobek, M.R., Bustos, C.A., Pfeifer, H.-R., 2014. Element cycling during the transition from alkaline to acidic environment in an active porphyry copper tailings impoundment, Chuquicamata, Chile. J. Geochem. Explor. 140, 23–40. https://doi.org/10.1016/j.gexplo.2014.01.013.

Song, X., Pettersen, J.B., Pedersen, K.B., Røberg, S., 2017. Comparative life cycle assessment of tailings management and energy scenarios for a copper ore mine: A case study in Northern Norway. J. Cleaner Prod. 164, 892–904.

Tapia, J.S., Valdés, J., Orrego, R., Tchernitchin, A., Dorador, C., Bolados, A., Harrod, C., 2018. Geologic and anthropogenic sources of contamination in settled dust of a historic mining port city in northern Chile: Health risk implications. PeerJ (San Francisco, CA) 6, e4699.

Taylor, M.P., Mould, S.A., Kristensen, L.J., Rouillon, M., 2014. Environmental arsenic, cadmium and lead dust emissions from metal mine operations: implications for environmental management, monitoring and human health. Environ. Res. 135, 296–303. https://doi.org/10.1016/j.envres.2014.08.036.

Tchounwou, P.B., Patlolla, A.K., Centeno, J.A., 2003. Invited reviews: carcinogenic and systemic health effects associated with arsenic exposure—a critical review. Toxicol. Pathol. 31 (6), 575–588. https://doi.org/10.1080/01926230390242007.

Thomas, L.D.K., Hodgson, S., Nieuwenhuijsen, M., Jarup, L., 2009. Early kidney damage in a population exposed to cadmium and other heavy metals. Environ. Health Perspect. 117 (2), 181–184.

Trujillo-González, J.M., Torres-Mora, M.A., Keesstra, S., Brevik, E.C., Jiménez-Ballesta, R., 2016. Heavy metal accumulation related to population density in road dust samples taken from urban sites under different land uses. Sci. Total Environ. 553, 636–642.

United States Environmental Protection Agency, 1989. Risk Assessment Guidance for Superfund, Vol I: Human Health Evaluation Manual. EPA/540/1–89/002 Office of Solid Waste and Emergency Response, Washington, DC.

United States Environmental Protection Agency, 2009. Highlights of the child-specific exposure factors handbook (final report). USEPA, Washington, DC EPA/600/R-08/135.

United States Environmental Protection Agency, 2013. Regional screening levels (RSL) for chemical contaminants at Superfund Sites. USEPA, Washington, DC.

Vergara, J.I., Gundermann, H., Foerster, R., 2006. Legalidad y legitimidad: Ley indígena, Estado chileno y pueblos originarios (1989–2004). Estudios Sociológicos 24 (71), 331.

Kolakkandi, V., Sharma, B., Rana, A., Dey, S., Rawat, P., Sarkar, S., 2020. Spatially resolved distribution, sources and health risks of heavy metals in size-fractionated road dust from 57 sites across megacity Kolkata, India. Sci. Total Environ. 705, 135805.

Vleeschouwer, F.D., Vanneste, H., Mauquoy, D., Piotrowska, N., Torrejón, F., Roland, T., Stein, A., Le Roux, G., Hart, J.P., 2014. Emissions from Pre-Hispanic Metallurgy in the South American Atmosphere. PLoS ONE 9 (10), e111315.

Watanabe, T., Hirano, S., 2013. Metabolism of arsenic and its toxicological relevance. Arch. Toxicol. 87 (6), 969–979. https://doi.org/10.1007/s00204-012-0904-5.

Wilson, S.T., Wang, H., Kabenge, M., Qi, X., 2017. The mining sector of Liberia: Current practices and environmental challenges. Environ. Sci. Pollut. Res. 24 (23), 18711–18720.

Yang, Q., Chen, H., Li, B., 2015. Source identification and health risk assessment of metals in indoor dust in the vicinity of phosphorus mining, Guizhou Province, China. Arch. Environ. Contam. Toxicol. 68 (1), 20–30. https://doi.org/10.1007/s00244-014-0064-0.

Yu, J., Yu, H., Xu, L., Tao, T., Zhang, Y., Hua, Y., Nkolola, N.B., 2017. Characteristic comparison of heavy metal contamination between road-deposited and roof-deposited sediments in suburban area. Environ. Sci. Pollut. Res. 24 (14), 12871–12881.

Zang, C., Dame, J., Nüsser, M., 2018. Hydrochemical and environmental isotope analysis of groundwater and surface water in a dry mountain region in Northern Chile. Environ. Monit. Assess. 190, 334. https://doi.org/10.1007/s10661-018-6664-9.

Zapata, G.Y.V., 2020. Problemas medioambientales de la minería aurífera ilegal en Madre de Dios (Perú). Observatorio Medioambiental 23, 229.

Zhao, N.i., Lu, X., Chao, S., 2016. Risk assessment of potentially toxic elements in smaller than 100-μm street dust particles from a valley-city in northwestern China. Environ. Geochem. Health 38 (2), 483–496.

Zhu, C., Tian, H., Hao, J., 2020. Global anthropogenic atmospheric emission inventory of twelve typical hazardous trace elements, 1995–2012. Atmos. Environ. 220, 117061 https://doi.org/10.1016/j.atmosenv.2019.117061.

Zhu, X.-S., Lu, M.-J., 2016. Regional metallogenic structure based on aeromagnetic data in northern Chile. Appl. Geophys. 13 (4), 721–735. https://doi.org/10.1007/s11770-016-0593-6.

Zografos, C., Robbins, P., 2020. Green Sacrifice Zones, or Why a Green New Deal Cannot Ignore the Cost Shifts of Just Transitions. One Earth 3 (5), 543–546. https://doi.org/10.1016/j.oneear.2020.10.012.